Lattice dynamics calculations and temperature dependence of vibrational modes of ferroelastic Li_2TiGeO_5

2006 J. Phys.: Condens. Matter 18 2137

(http://iopscience.iop.org/0953-8984/18/7/003)

INSTITUTE OF PHYSICS PUBLISHING JOURNAL OF PHYSICS: CONDENSED MATTER

J. Phys.: Condens. Matter **18** (2006) 2137–2147 doi:10.1088/0953-8984/18/7/003

Lattice dynamics calculations and temperature dependence of vibrational modes of ferroelastic Li_2TiGeO_5

M Mączka[1], A Sieradzki[2], R Poprawski[2], K Hermanowicz[1] and J Hanuza[1,3]

[1] Institute of Low Temperature and Structure Research, Polish Academy of Sciences, PO Box 1410, 50-950 Wrocław 2, Poland
[2] Institute of Physics, Wrocław University of Technology, Wybrzeże, Wyspiańskiego 27, 50-370 Wrocław, Poland
[3] Department of Bioorganic Chemistry, Faculty of Industry and Economics, Wrocław University of Economics, 118/120 Komandorska Street, 53-345 Wrocław, Poland

Received 12 December 2005, in final form 6 January 2006
Published 30 January 2006
Online at stacks.iop.org/JPhysCM/18/2137

Abstract

Raman and polycrystalline IR spectra were obtained for Li_2TiGeO_5 and the assignment of the observed bands to the respective internal and external phonons has been proposed on the basis of lattice dynamics calculations. Temperature dependences of Raman- and IR-active phonons are also reported to probe the paraelastic–ferroelastic phase transition that takes place at 233.5 K. This study shows that the phase transition is continuous and that this phase transition leads to significant distortion of the unit cell.

1. Introduction

A considerable interest in the studies of titanium-containing crystalline compounds is associated with their valuable physical properties, of which very important are the nonlinear optical properties. The crystals with the general formula A_2TiMO_5 (where A = Li or Na and M = Ge or Si) have a layered structure, in which the main layers of Ti semioctahedra and M tetrahedra alternate with interlayers of mobile cations of alkali metals. Crystals of lithium titanium germanate (Li_2TiGeO_5) were first discovered by Bastow *et al* [1]. They crystallize at room temperature in a tetragonal perovskite-like structure with symmetry $P4/nmm$. The crystal structure consists of layers of GeO_4 tetrahedra and TiO_5 square pyramids joined by shared corners. These layers of $[TiGeO_5]^{2-}$ anions are separated by layers of lithium ions. The layered structure creates a large anisotropy in the physical properties; for instance the ratio of the electric conductivity along the *a* and the *c* axes is of the order 10^3–10^4 [2].

Calorimetric, dilatometric, electrical, and linear birefringence measurements have shown that there is a ferroelastic phase transition at 233.5 K [3, 4]. Below the ferroelastic phase

transition point ($T_c = 233.5$ K) the tetragonal lattice is distorted and the crystal becomes orthorhombic (symmetry $Pmmn$) [5].

In the present paper we report lattice dynamics calculations and temperature dependent IR and Raman studies in order to get some insight into the nature of the observed modes and the mechanism of the ferroelastic phase transition occurring at 233.5 K. We would like to emphasize that the phonon properties of this material have not yet been studied and the mechanism of the phase transition has not yet been explained.

2. Experiment

Single crystals were grown by a flux method in a hemispherical platinum bowl. A mixture of 80% $LiMoO_4$ and 20% Li_2WO_4 was used as a solvent. The weight ratio of the Li_2TiGeO_5 mixture and the solvent was 6:5. The crystallization was performed by cooling from the temperature of about 1250–1230 K with the rate of 0.05 K h^{-1}. The details of crystallization were described in paper [2].

Polycrystalline infrared spectra were measured from the grounded crystals with a Biorad 575C FT-IR spectrometer in KBr suspension for the 1200–400 cm^{-1} region and in Nujol suspension for the 500–30 cm^{-1} region. Polarized spectra of a single crystal were measured with a Biorad 575C FT-IR spectrometer using a fixed angle specular reflectance accessory. FT-Raman spectra were measured for an oriented single crystal using a Bruker 110/S spectrometer with YAG:Nd^{3+} excitation. Temperature-dependent studies of IR spectra in the 10–300 K temperature range were performed using a helium-flow Oxford cryostat. Temperature-dependent Raman spectra in the 100–300 K region were measured using a Linkam cryostat cell (THMS 600). Both IR and Raman spectra were recorded with a spectral resolution of 2 cm^{-1}.

3. Results and discussion

3.1. Room temperature Raman and IR spectra

First the symmetry and vibrational properties of the room-temperature $P4/nmm$ structure of Li_2TiGeO_5, presented in figure 1, will be described in order to establish the basis for discussing the temperature dependent Raman and IR results. For this tetragonal structure, group theory predicts $4A_{1g} + A_{2g} + 3B_{1g} + B_{2g} + 6E_g + 2A_{1u} + 7A_{2u} + 3B_{1u} + 3B_{2u} + 9E_u$ Brillouin zone centre modes. These modes can be further subdivided into $3A_{1g} + A_{2g} + 2B_{1g} + B_{2g} + 4E_g + A_{1u} + 3A_{2u} + B_{1u} + 2B_{2u} + 4E_u$ stretching and bending vibrations of the GeO_4 and TiO_5 groups, $A_{1g} + E_g + A_{2u} + E_u$ translations of Ti^{4+} ions, $B_{1g} + E_g + A_{2u} + E_u$ translations of Ge^{4+} ions and $A_{1u} + 2A_{2u} + 2B_{1u} + B_{2u} + 3E_u$ translations of Li^+ ions. It should be remembered, however, that among translational modes two modes (A_u and E_u) belong to acoustic branches. Among these modes A_{1g}, B_{1g}, B_{2g} and E_g modes are Raman active and A_{2u} and E_u modes are IR active whereas the A_{2g}, A_{1u}, B_{1u} and B_{2u} modes are both IR and Raman inactive. This analysis shows that one expects to observe 14 modes both in IR and Raman spectra.

Room-temperature Raman spectra of the single Li_2TiGeO_5 crystal measured in different polarization configurations are shown in figure 2. This figure shows that out of 14 expected Raman modes only 10 modes can be observed. The smaller number of observed modes can be most likely attributed to the very weak intensity of some modes and/or accidental similarity in frequencies of some modes. Although the Raman spectra are not very well polarized, the comparison of the spectra measured in different polarization configurations allows us to conclude that the bands near 824, 725 and 519 cm^{-1} correspond to the modes of A_{1g} symmetry.

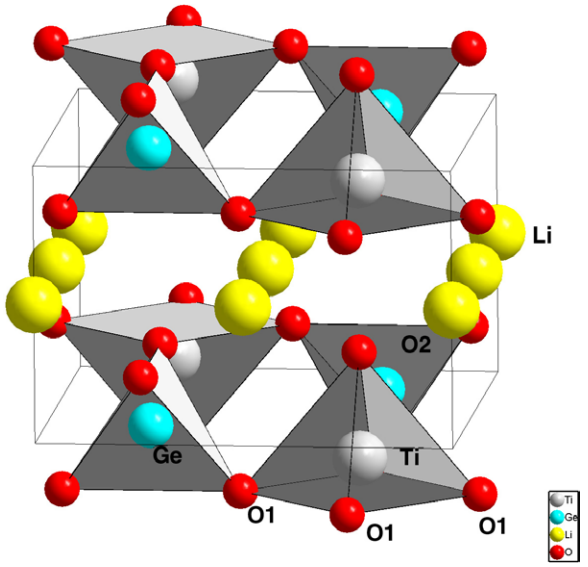

Figure 1. View of the crystal structure of Li_2TiGeO_5.
(This figure is in colour only in the electronic version)

The E_g modes are observed at 743, 488, 401, 265 and 209 cm^{-1} since these modes have highest intensity in the $y(xz)\bar{y}$ polarization. The mode at 215 cm^{-1} is clearly seen only in the $y(zz)\bar{y}$ polarization as a shoulder on the 209 cm^{-1} band and can, therefore, be assigned to A_{1g} symmetry. The lowest frequency mode at 142 cm^{-1} has the strongest intensity in the $y(xx)\bar{y}$ polarization and can be most likely assigned to B_{1g} symmetry.

Figure 3 presents the IR spectrum measured for the single crystal. The IR reflection spectrum was recorded with polarization parallel to the x-axis only since due to pronounced cleavage of the crystals the dimension along the z-axis was very small. In this polarization only E_u modes should be observed. This spectrum was fitted by using a four-parameter model [6] in order to give information about TO and LO wavenumbers. According to this model, the complex dielectric constant is expressed in terms of the IR-active modes as follows:

$$\varepsilon(\omega) = \varepsilon_\infty \prod_j \frac{\omega_{j\mathrm{LO}}^2 - \omega^2 + \mathrm{i}\omega\gamma_{j\mathrm{LO}}}{\omega_{j\mathrm{TO}}^2 - \omega^2 + \mathrm{i}\omega\gamma_{j\mathrm{TO}}} \tag{1}$$

where $\omega_{j\mathrm{TO}}$ and $\omega_{j\mathrm{LO}}$ correspond to the resonance wavenumbers of the jth transversal and longitudinal modes, respectively, and $\gamma_{j\mathrm{TO}}$ and $\gamma_{j\mathrm{LO}}$ are the corresponding damping factors. ε_∞ is the dielectric constant. For normal incidence, the infrared reflectivity R and the dielectric function are related by

$$R = \left| \frac{\sqrt{\varepsilon} - 1}{\sqrt{\varepsilon} + 1} \right|^2 . \tag{2}$$

The results of fitting of the experimental data to the four-parameter model are summarized in table 1, where oscillator strengths $\Delta\varepsilon_{\mathrm{TO}}$ are also given.

The reflection spectrum shows the presence of seven E_u modes in the 1000–200 cm^{-1} region (see table 1). The polycrystalline spectrum, presented in figure 4, shows in this frequency region a few more bands at 899, 847, 553, 491, 452 and 322 cm^{-1}, which can be attributed to the A_{2u} symmetry. The polycrystalline spectrum also shows the presence of two bands at

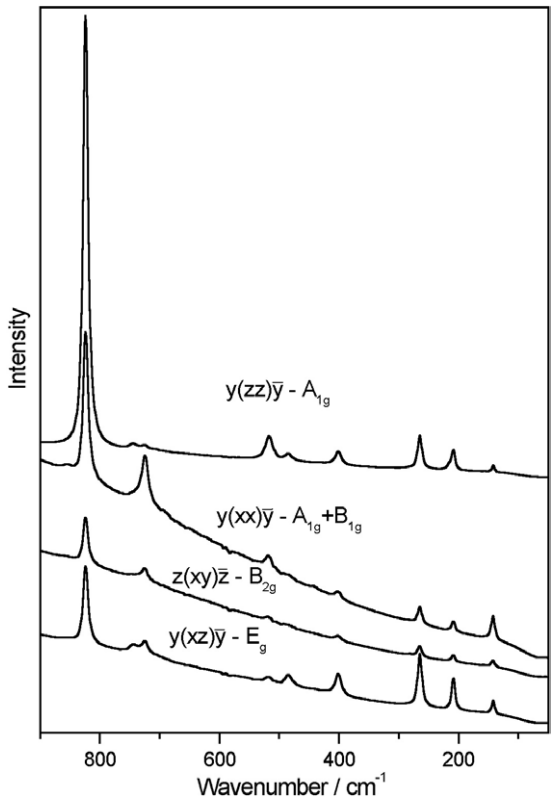

Figure 2. Polarized Raman spectra of Li_2TiGeO_5.

Table 1. Dispersion parameters for the best fit to the reflectivity data for E $\parallel$ x polarization.

ω_{TO} (cm^{-1})	γ_{TO} (cm^{-1})	ω_{LO} (cm^{-1})	γ_{LO} (cm^{-1})	$\Delta\varepsilon_{TO}$
299.0	32.3	306.3	31.4	0.553
339.3	15.2	353.0	22.5	0.861
366.0	20.8	381.2	16.8	0.408
405.4	40.4	445.1	194.8	0.535
517.1	52.3	548.4	45.1	0.319
709.7	70.4	709.8	49.3	0.001
746.6	55.7	832.8	196.9	0.648
		$\varepsilon_\infty = 2.81$		

227 and 125 cm^{-1}. Since the intensity of the 227 cm^{-1} mode is very low and the reflection spectrum below 240 cm^{-1} is noisy, it is not clear whether this mode appears in the reflection spectrum or not. On the other hand, the reflection spectrum could not be recorded below 200 cm^{-1}. We cannot, therefore, conclude what symmetry should be attributed to these two low frequency modes.

3.2. Lattice dynamics calculations and assignment of modes

In order to adequately assign the Raman and IR peaks to the atomic vibrations, we performed lattice dynamics calculations. Since Li_2TiGeO_5 is mostly ionic, we performed the calculations

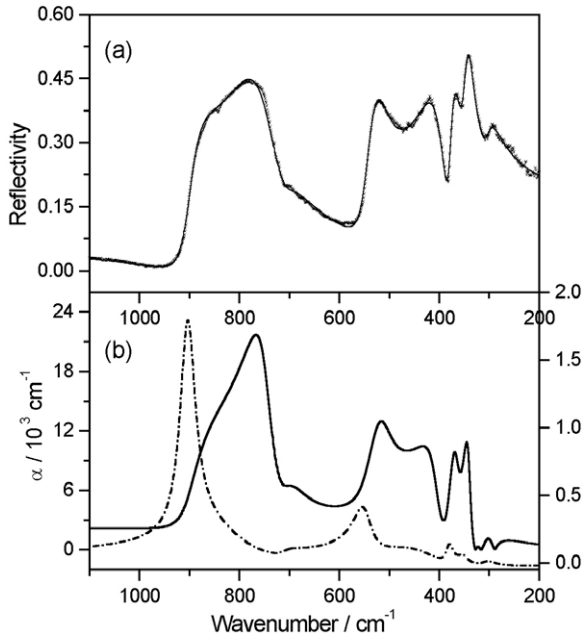

Figure 3. (a) Infrared reflectivity data for $E \parallel x$ polarization (crosses) and the best fit by the four-parameter model (solid line). (b) Calculated wavenumber dependence of the absorption coefficient (solid line) and imaginary part of the inverse dielectric function (dotted line).

on the basis of a partially ionic model described in the paper by Nozaki *et al* [7]. The atomic positions used in the calculations were taken from [2]. The following interatomic potential was used in the lattice dynamics calculations:

$$U_{ij}(r_{ij}) = \frac{z_i z_j e^2}{r_{ij}} + (b_i + b_j)\exp\left[\frac{a_i + a_j - r_{ij}}{b_i + b_j}\right] - \frac{c_i c_j}{r_{ij}^6} + D_{ij}(\exp[-2\beta_{ij}(r_{ij} - r_{ij}^*)] - 2\exp[-2\beta_{ij}(r_{ij} - r_{ij}^*)]). \quad (3)$$

This interatomic potential consists of a Coulomb interaction (first term) to model the long-range interactions; a Born–Mayer type repulsive interaction (second term) to account for the short-range forces; a van der Waals attractive interaction (third term) to model the dipole–dipole interaction and finally the Morse potential contribution (last term) to take into account the covalent bond character. z_i and z_j are the effective charges of ions i and j, respectively, separated by the distance r_{ij}. The parameters (a_i, a_j) and (b_i, b_j) correspond to the ionic radii and ionic stiffness, respectively. The values of the parameters for the oxygen, lithium and titanium ions were taken from [7]. The values of the parameter for germanium were the same as those used in lattice dynamics calculations for GeO_2 [8]. Some of the initial parameters were changed during the calculations in small steps in order to obtain the best agreement between the observed and calculated wavenumbers. The parameters used in the present calculations are listed in table 2. Since we consider covalency for the Ti–O bond only, D_{ij}, β_{ij} and r_{ij}^* are given for this bond. The calculated and experimental frequencies are shown in table 3.

The obtained results show that the spectra are clearly divided into two regions: 700–900 and 100–560 cm^{-1}. Since the performed calculations give not only mode frequencies but also displacement of atoms for every calculated mode, we may assign on this basis the

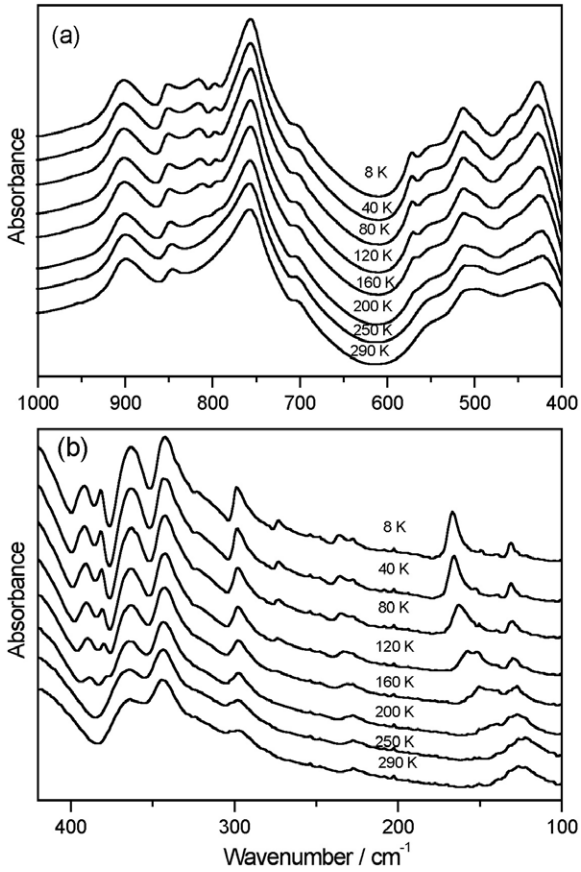

Figure 4. Polycrystalline IR spectra in the (a) mid-IR and (b) far-IR region, measured at different temperatures.

Table 2. Potential parameters used for the lattice dynamics calculations.

ith ion	z_i (e)	a_i (Å)	b_i (Å)	C (kcal$^{1/2}$ Å^3 mol$^{-1/2}$)
Li	0.7	0.954	0.09	5
Ti	1.8	1.079	0.10	0
Ge	1.8	0.868	0.09	0
O	−1.0	1.926	0.16	20
Ion pair	D_{ji} (kcal mol^{-1})	β_{ij} (Å)	r^*_{ij} (Å)	
Ti–O	24.0	1.9	1.8	

modes to respective motions of atoms in the unit cell. The calculations reveal that the higher frequency modes correspond to stretching modes of Ge–O and Ti–O bonds whereas the modes in the lower frequency region correspond to bending and lattice modes. They show that the highest frequency A_{1g} Raman mode observed (calculated) at 824(885) cm^{-1} and IR mode at 899 (879) cm^{-1} can be assigned to stretching vibrations of the short Ti–O2 bond which projects into the layer space, as shown in figure 1. A very similar stretching mode was observed near 865–875 cm^{-1} in Raman spectra of $M_2La_2Ti_3O_{10}$ (M = Li, Na, Rb) layered titanates [7],

Table 3. Observed and calculated wavenumbers (in cm^{-1}) for Raman (A_{1g}, B_{1g}, B_{2g}, E_g) and IR (A_{2u} and E_u) modes of Li_2TiGeO_5 together with the proposed assignment (in the case when assignments for IR and Raman modes are different, the former is written in bold characters). For the IR-active modes the LO wavenumbers are given in parentheses. (Note: ν and δ denote stretching and bending vibrations, respectively. T′(Li), T′(Ti) and T′(Ge) denote translations of Li^+, Ti^{4+} and Ge^{4+} ions, respectively. '*' denotes coupling. s, m, w and sh denote strong, medium, weak and shoulder.)

Raman			IR			
Obs.	Calc.	Symmetry	Obs.	Calc.	Symmetry	Assignment
824s	885	A_{1g}	899m	879 (910)	A_{2u}	ν(Ti–O2)
	619	B_{2g}	847w	728 (730)	A_{2u}	ν(Ge–O1–Ti)
743w	612	E_g	755s	608 (665)	E_u	ν (Ge–O1–Ti)
725w	765	A_{1g}				ν(Ge–O1–Ti)
519w	586	A_{1g}	553sh	535 (660)	A_{2u}	δ(Ge–O10–Ti) +δ(**Ge–O1–Ti**)*T′(**Li**)
488w	502	E_g	513m	521 (605)	E_u	δ(Ge–O1–Ti) + δ(**Ge–O1–Ti**)*T′(**Li**)
	506	B_{1g}	452sh	437 (506)	A_{2u}	δ(Ge–O1–Ti) + δ(**Ge–O1–Ti**)*T′(**Ti**)
401w	444	E_g	416s	442 (515)	E_u	δ(Ge–O1–Ti) + T′(**Li**)
	324	B_{1g}	365w	430 (431)	E_u	δ(Ge–O1–Ti)
265m	274	E_g	343s	403 (411)	E_u	T′(Ti) + δ(**Ge–O1–Ti**)
215sh	245	A_{1g}	322sh	303 (308)	A_{2u}	T′(Ti) + T′(**Li**)
209m	215	E_g	296w	302 (312)	E_u	T′(Ti)
			—	168 (206)	A_{2u}	T′(Ge)
	154	E_g	227w	206 (252)	E_u	T′(Ge)
142w	137	B_{1g}	125m	123 (180)	E_u	T′(Ge) + δ(**Ti–O2**)*T′(**Li**)

although Li_2TiGeO_5 and $M_2La_2Ti_3O_{10}$ compounds have significantly different structures, i.e. in the former compound TiO_5 groups are present whereas in the latter titanium coordination is octahedral. The remaining stretching modes correspond to vibrations of the O1 oxygen atom, which connects TiO_5 and GeO_4 polyhedra via a Ti–O1–Ge bridge. Vibrations of the Ge–O–Ge bridge were observed at 698 cm^{-1} for Li_2GeO_3 [9, 10] and near 800–860 cm^{-1} for $Li_2Ge_7O_{15}$ [11]. It is also worth noting that the calculations predict the presence of only one E_u and two A_{2u} modes in the high-frequency region whereas two E_u modes were observed in the reflection spectra (see tables 1 and 3). The origin of the weak E_u mode, observed at 710 cm^{-1}, is not clear.

The assignment of the modes below 560 cm^{-1} is less certain since many modes in this region have similar frequencies and may couple each to other. Nevertheless, the calculations show that the Raman bands observed at 401, 488 and 519 cm^{-1} can be assigned to bending vibrations of the Ge–O1–Ti bridges. The Raman bands at 215, 209 and 265 cm^{-1} have a very large contribution of Ti^{4+} translational motions and the modes at 142 cm^{-1} can be assigned to translations of Ge^{4+} ions. The IR-active Ge–O1–Ti modes are observed in the 340–560 cm^{-1} range. However, our calculations suggest that the modes observed at 553 and 513 cm^{-1} have also a significant contribution of Li^+ motions, i.e. these modes should be classified as coupled T′(Li) translational and Ge–O-Ti bending vibrations. Similarly, the mode observed at 452 cm^{-1} has significant contribution of Ti^{4+} motions and should be assigned to coupled T′(Ti) translational and Ge–O-Ti bending vibration. Translations of Li^+ ions are also predicted to be observed near 416 (442) and 322 (303) cm^{-1}. The region of T′(Li) modes predicted by our calculations is in good agreement with the previous studies of Li_2GeO_3 where these modes were located in the 250–500 cm^{-1} region on the basis of isotopic substitution [10]. Translational motions of Ti^{4+} and Ge^{4+} ions are expected to contribute significantly to those IR modes which are observed at 296 and 227 cm^{-1}, respectively. Finally, the performed calculations show that

Table 4. The correlation diagram showing the correspondence between the optical modes in the $P4/nmm$ and $Pmmn$ structures of Li_2TiGeO_5 (the data for the $Pmmn$ structure are given in parentheses). The modes which should become active in the $Pmmn$ structure are written in bold characters.

Ion	Site symmetry	Factor group symmetry
Ti and O2	$C_{4v}(C_{2v})$	$D_{4h}(D_{2h})$
	$A_1(A_1)$	$A_{1g}(A_g)$
		$A_{2u}(B_{1u})$
	$E\ (B_1 + B_2)$	$E_g(B_{2g} + B_{3g})$
		$E_u(B_{2u} + B_{3u})$
Ge	$D_{2d}(C_{2v})$	$D_{4h}(D_{2h})$
	$B_2(A_1)$	$B_{1g}(A_g)$
		$A_{2u}(B_{1u})$
	$E\ (B_1 + B_2)$	$E_g(B_{2g} + B_{3g})$
		$E_u(B_{2u} + B_{3u})$
Li	$C_{2h}(C_i)$	$D_{4h}(D_{2h})$
	$A_u(A_u)$	$A_{1u}(A_u)$
		$B_{2u}(\mathbf{B_{1u}})$
		$E_u(B_{2u} + B_{3u})$
	$2B_u(2A_u)$	$2A_{2u}(2B_{1u})$
		$2B_{1u}(2A_u)$
		$2E_u(2B_{2u} + 2B_{3u})$
O1	$C_s(C_s)$	$D_{4h}(D_{2h})$
	$A''(2A'')$	$A_{2g}(\mathbf{B_{1g}})$
		$B_{2g}(B_{1g})$
		$E_g(B_{2g} + B_{3g})$
		$A_{1u}(A_u)$
		$B_{1u}(A_u)$
		$E_u(B_{2u} + B_{3u})$
	$2A'(4A')$	$2A_{1g}(2A_g)$
		$2B_{1g}(2A_g)$
		$2E_g(2B_{2g} + 2B_{3g})$
		$2A_{2u}(2B_{1u})$
		$2B_{2u}(2\mathbf{B_{1u}})$
		$2E_u(2B_{2u} + 2B_{3u})$

the lowest frequency IR mode, observed at 125 cm^{-1}, involves large contributions of Li and O2 ions vibrations.

3.3. Temperature dependence of IR and Raman modes

Once a clear picture of the vibrational properties of the tetragonal phase of Li_2TiGeO_5 are obtained we next discuss the effects of temperature on the vibrational properties of this compound. Our previous studies showed that this crystal exhibits a second order, ferroelastic phase transition at $T_c = 233.5$ K [4, 5]. The x-ray studies revealed that below the phase transition temperature the crystal is orthorhombic (space group $Pmmn$) [5]. The number of ions in the unit cell does not change during the transition. As a result of the $P4/nmm$ to $Pmmn$ phase transition the site symmetry of Ti, Ge, Li and O2 decreases from C_{4v}, D_{2d}, C_{2h} and C_{4v} to C_{2v}, C_{2v}, C_i and C_{2v}, respectively [5]. The site symmetry of O1 ions remains C_s in both phases but these ions become distributed into two nonequivalent sites in the $Pmmn$ structure.

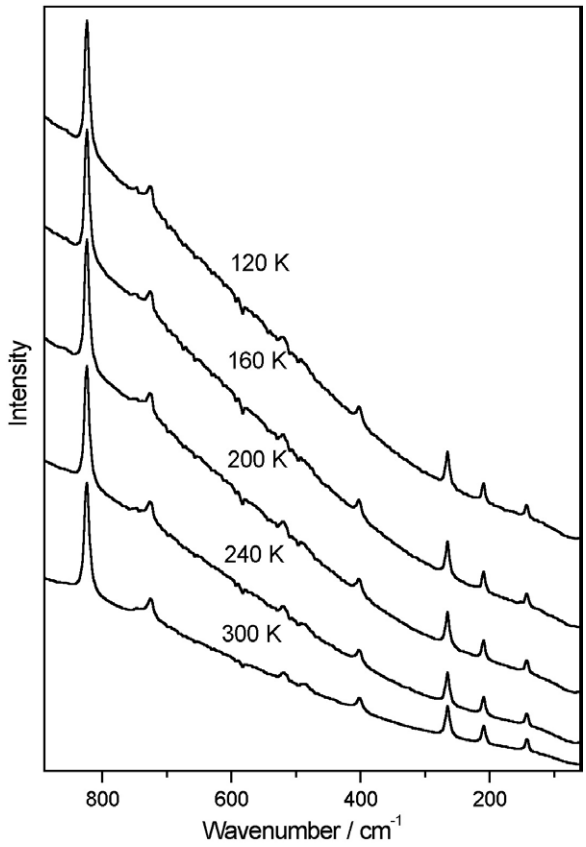

Figure 5. Raman spectra of Li_2TiGeO_5 recorded at different temperatures in $z(xx + xy)z$ polarization.

Group theoretical analysis shows that as a result of the $P4/nmm$ to $Pmmn$ phase transition all E_g and E_u modes should split into doublets (see table 4). Moreover, three B_{2u} modes and one A_{2g} mode of the $P4/nmm$ structure, which are both IR and Raman inactive, should become active below the phase transition either in IR or Raman spectroscopy (see table 4).

Our results show that temperature dependent changes in the Raman spectra are very weak (see figure 5). In particular, no splitting of the doubly degenerated modes can be observed, and any new mode which corresponds to the A_{2g} mode of the $P4/nmm$ structure cannot be observed below T_c. The changes in the IR spectra are much more pronounced (see figures 4 and 6). In particular, a few new modes appear at 812, 795, 571, 389, 379 and 273 cm^{-1}, and the 227 and 125 cm^{-1} bands split into doublets below T_c. The observation of splitting for the lowest frequency modes indicates that these modes have E_u symmetry in the paraelastic phase. The appearance of new modes could be due to splitting of the E_u modes and/or activation of the B_{2u} modes of the $P4/nmm$ phase. Our lattice dynamics calculations predict that the B_{2u} modes should be observed near 657 cm^{-1} (Ge–O1–Ti stretching mode), 516 cm^{-1} (Ge–O1–Ti bending mode) and 441 cm^{-1} (T′(Li) translational mode). Since the calculated frequency of the B_{2u} stretching mode is about 50 cm^{-1} higher than the calculated frequency of the E_u stretching mode (see table 3), this mode should be observed near 800 cm^{-1}. We may assign, therefore, either the 812 or 795 cm^{-1} band to the B_{2u} mode. The second band should be then

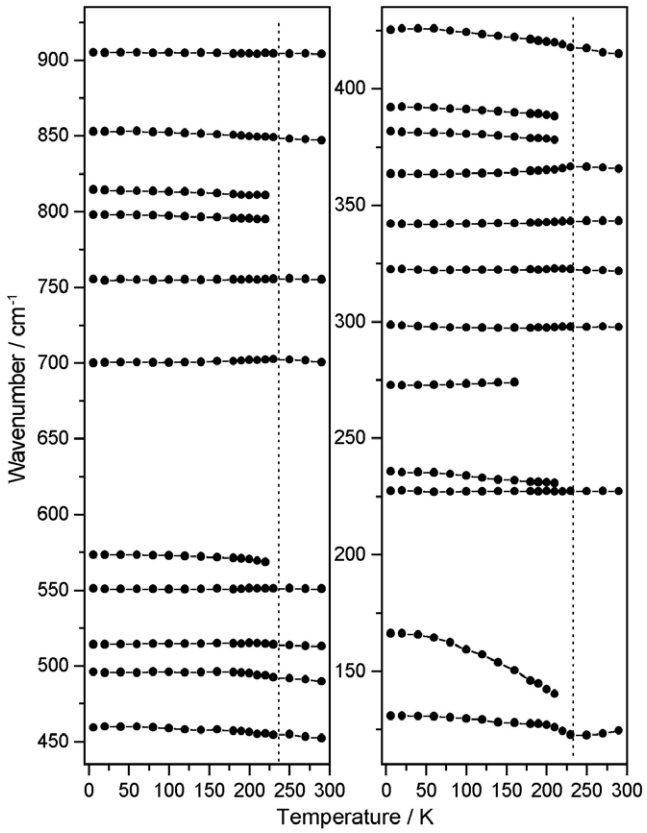

Figure 6. IR frequency versus temperature plot. The solid lines are to guide the eye. The vertical lines indicate the temperature at which the phase transition takes place.

assigned to splitting of the 755 cm^{-1} E_u mode. In a similar way, the appearance of the 571 and 389 cm^{-1} bands below T_c can be attributed to activation of the B_{2u} modes, calculated at 516 and 441 cm^{-1}, or splitting of the 513 and 416 cm^{-1} modes. The 379 and 273 cm^{-1} bands appear as a result of splitting of the 365 and 296 cm^{-1} modes.

It is worth noting that intensity of the new modes, appearing below the phase transition temperature, increases continuously with decreasing temperature, in agreement with the second-order character of this transition. The observation of relatively large splitting of E_u modes indicates significant distortion of the unit cell from its tetragonal symmetry at the lowest temperatures. It is surprising that the Raman spectra do not show any noticeable changes in the 120–230 K range although IR spectra show very clearly the onset of the phase transition. The origin of this behaviour is not clear. It should, however, be noticed that Raman-active modes do not involve vibrations of Li^+ ions, whereas vibrational motions of Li^+ ions participate significantly in many IR-active modes. It is, therefore, likely that observation of significant changes in the IR spectra as a function of temperature may indicate that some important changes occur within the layer formed of Li^+ ions. It is worth noting that our recent heat capacity study suggested an order–disorder mechanism of the phase transition [4]. Our present results suggest that ordering of Li^+ ions may play an important role below T_c. The ordering of Li^+ ions as a mechanism of phase transition in Li_2TiGeO_5 is likely since this type of

order–disorder phase transition was observed in other lithium germanates such as $LiNaGe_4O_9$ and $Li_2Ge_7O_{15}$ [11, 12].

4. Conclusions

The performed studies allowed us to establish symmetry of the observed vibrational modes and propose assignment of observed modes to respective vibrations of structural units. The measured IR spectra show very clearly the onset of the 233.5 K phase transition through splitting of the E_u modes and activation of new modes which were inactive in the paraelastic phase. The character of the observed changes in the IR spectra confirms that the phase transition is continuous. Our results also suggest that this transition may be connected with significant changes within the Li^+ layers, possibly ordering of Li^+ ions below T_c.

References

[1] Bastow T J, Botton G A, Etheridge J, Smith M E and Whitfield H J 1999 *Acta Crystallogr.* A **55** 127
[2] Kireev V V, Yakubovich O V, Ivanov-Shitz A K, Melnikov O K, Demyanets L N, Skunman J and Chaban N G 2001 *Russ. J. Coord. Chem.* **27** 31
[3] Poprawski R, Przesławski J, Kireev V V, Schaldin Yu V and Just M 2001 *Phys. Status Solidi* a **183** R7
[4] Przesławski J, Poprawski R, Just M, Kireev V V, Mielcarek S and Mróz B 2002 *Ferroelectrics* **267** 201
[5] Sieradzki A, Poprawski R and Pietraszko A 2004 *Phase Transit.* **77** 289
[6] Gervais F and Echegut P 1986 *Incommensurate Phases in Dielectrics* ed R Blinc and A P Levanyuk (Amsterdam: North-Holland) p 337
[7] Nozaki R, Kondo J N, Hirose C, Domen K, Wada A and Morioka Y 2001 *J. Phys. Chem.* B **105** 7950
[8] Tsuchiya T, Yamanaka T and Matsui M 1998 *Phys. Chem. Minerals* **25** 94
[9] Xu Y, Li Y and Lan G 1996 *Spectrochim. Acta* A **52** 1417
[10] Orel B, Klanjsek M, Moiseenko V, Volnyanskii M, Le Calve N, Pasquier B and Novak A 1985 *Phys. Status Solidi* b **128** 53
[11] Torgashev V, Yuzyuk Yu, Latush L, Burmistrova L, Kadlec F, Smutny F and Petzelt J 1995 *J. Phys.: Condens. Matter* **7** 5681
[12] Buixaderas E, Kamba S, Gregora I, Vanek P, Petzelt J, Yamaguchi T and Wada M 1999 *Phys. Status Solidi* b **214** 441